

## Quantum-well anisotropic forbidden transitions induced by a common-atom interface potential

Y. H. Chen and Z. Yang

*Department of Physics, Hong Kong University of Science and Technology, Clearwater Bay, Kowloon, Hong Kong, China*

Z. G. Wang, Xu Bo, and J. B. Liang

*Laboratory of Semiconductor Materials Science, Institute of Semiconductors, Chinese Academy of Sciences, Box 912, Beijing 100083, China*

(Received 26 January 1999)

A prominent effect of the interface potential (IP) [E. L. Ivchenko and A. Yu. Kaminski, *Phys. Rev. B* **54**, 5852 (1996); O. Krebs and P. Voisin, *Phys. Rev. Lett.* **77**, 1829 (1996)], the optical anisotropy of the forbidden transitions in quantum wells has been observed by reflectance-difference spectroscopy. Predictions by the heavy-light-hole coupling IP models are qualitatively consistent with all the observed features of the forbidden and the allowed transitions. The fact that the predicted value of the relative transition strength, which depends on neither the IP strength nor the electric field, disagrees with the observed one indicates that coupling involving  $X$  and/or  $L$  bands may also be important. [S0163-1829(99)04227-7]

Due to the difference of chemical bonds along the  $[110]$  and the  $[1\bar{1}0]$  directions, (100) oriented semiconductor interfaces are expected to be anisotropic.<sup>1-5</sup> Indeed, strong optical anisotropy was observed recently and was attributed to this intrinsic anisotropy of the interfaces with no common atoms.<sup>3-5</sup> Based on the tight-binding theory, perturbation Hamiltonian arising from the anisotropy of interface has been derived. Such interface potential (IP) can then be included in the  $\mathbf{K}^*\mathbf{P}$  theory for the optical properties of quantum wells (QW's) and superlattices (SL's).<sup>1,2,6</sup> However, for common-atom interfaces, so far there are few experimental data that would allow detailed quantitative analysis of the IP. Krebs *et al.* recently reported the electric field-induced in-plane anisotropic absorption spectra of  $\text{In}_x\text{Ga}_{1-x}\text{As}/\text{InP}$  QW's. They showed that the observed anisotropy of the allowed transitions were largely due to the IP, and that the IP strength depends on the degree interface perfection.<sup>8</sup> In this paper, we show that a prominent effect of the IP is to induce optical anisotropy of the forbidden transitions in QW's, and report our quantitative analysis of the in-plane optical anisotropy of an (100)-oriented  $\text{In}_x\text{Ga}_{1-x}\text{As}/\text{GaAs}$  QW in a built-in small electric field ( $\sim 4.6$  KV/cm) measured by reflectance-difference spectroscopy (RDS). In the RD spectra of this sample, five anisotropic structures related to the different transitions of the QW, including two forbidden transitions and three allowed ones, are observed. The strong anisotropy and the line shape of the forbidden transitions, which cannot be explained by the conventional QW Pockels effect, can be qualitatively explained by the IP models.<sup>1,2</sup> More quantitative analysis, however, shows that the present IP models, which include only the coupling between the heavy-hole and the light-hole bands at the  $\Gamma$  point, are insufficient to explain the experimental data, and the complete IP may also include coupling involving higher bands at other critical points.

The IP derived by Ivchenko and Kaminski,<sup>1</sup> and by Krebs and Voisin<sup>2</sup> for (100) interfaces have the same form

$$V_{\text{int}} = -P_0(\hat{L}_x\hat{L}_y + \hat{L}_y\hat{L}_x)[\delta(z+a/2) - \delta(z-a/2)], \quad (1)$$

for a QW in  $-a/2 \leq z \leq a/2$ . Here  $\hat{L}_x$  and  $\hat{L}_y$  are the angular momentum operators, and  $\pm a/2$  represents the locations of the two interfaces of the QW. For Ivchenko's model  $P_0 = \hbar^2 t_{lh}/m_0 a_0$ , where  $m_0$  is the mass of free electron,  $a_0$  is the lattice constant, and  $t_{lh}$  is the heavy-light-hole mixing coefficient, which is estimated to be in the range of 0.3–0.9 for a GaAs/AlAs interface. For Krebs model,  $P_0 = 0.14a_0 e \Delta V$ , where  $\Delta V$  is valance band offset (VBO) at the interface.

The interface anisotropy potential given by Eq. (1) can be treated as a perturbation to the QW subband states, because the energy shift it causes is less than 1 meV for a typical QW of 70 Å wide. Therefore it has little effects on the normal optical properties, such as the subband energies and the strength of the allowed transitions. The IP does introduce optical anisotropy within the plane of the QW, but only if the QW is asymmetric, since the contribution of the IP of one QW boundary cancels out the other exactly when the QW is symmetric. The asymmetry can be introduced by a small external electric field perpendicular to the QW plane. The electric field, treated as a perturbation here,<sup>7</sup> couples the heavy hole (HH) and the light hole (LH) subbands of the same parity through the Pockels effect, because the uniform field itself is an even function. Such coupling causes in-plane anisotropy of the allowed transitions,  $\Delta M \equiv M_{[110]} - M_{[1\bar{1}0]}$ , where  $M_{[110]}$  and  $M_{[1\bar{1}0]}$  denote the optical transition intensity for light polarized along the  $[110]$  and the  $[1\bar{1}0]$  directions, respectively, regardless of the presence of the IP, and is known as the QW Pockels effect.<sup>7</sup> The strength of the in-plane anisotropy of the forbidden transitions induced by the field, without the IP effects, is much smaller, being  $\sim F^3$  as compared to  $\sim F$  for the allowed transitions. This is because the forbidden transitions involve subbands of different parities. To induce the transition, the wave functions must be distorted first, which gives rise to the  $\sim F^2$  dependence. The anisotropy is proportional to  $F$  so the final transition anisotropy is proportional to  $F^3$ .

The IP, being an odd function of space, couples the HH and LH subbands with different parities. For example, the IP

couples the 1L and the 2H (second heavy hole) subbands so that the perturbed 2H subband wave function now contains a small portion of the unperturbed  $|1L\rangle$  one. The 2H to 1C forbidden transition now becomes slightly allowed, because of the nonzero overlapping integral between the unperturbed  $|1C\rangle$  and the  $|1L\rangle$  states. However, its intensity is so low that it is very difficult to distinguish it from others induced by residual field or interface defects/roughness. The transition anisotropy is proportional to  $\langle 1C|1L\rangle\langle 1L|V_{int}|2H\rangle\langle 1C|2H\rangle$ . Since  $\langle 1C|2H\rangle=0$  at  $F=0$ , no optical anisotropy exists for symmetric QW's. When a small electric field is applied, the overlapping integral between the  $|2H\rangle$  and the  $|1C\rangle$  states becomes non-zero. In the transition anisotropy term,  $\langle 1C|1L\rangle\langle 1L|V_{int}|2H\rangle\langle 1C|2H\rangle$ , the first integral is nearly a constant, the second is proportional to the IP strength, and the last integral is proportional to  $F$ . In the presence of the IP, therefore, the anisotropy strength,  $\Delta M$ , is proportional to  $F$ , and can be much larger than the normal QW Pockels effect for the forbidden transitions. Similarly, the original  $\Delta M$  of the allowed transitions due to QW Pockels Effect will also be modified by the IP. As will be shown below, the value of  $\Delta M$  is of the order of  $10^{-4}$  for both the allowed and the forbidden transitions, while the value of  $M$  of the forbidden transitions are much smaller than the allowed ones. The IP effects could therefore be much better manifested in polarization sensitive optical experiments such as RDS (Refs. 3 and 9) where the anisotropy strength of both the allowed and the forbidden transitions are comparable.

An  $\text{In}_{0.2}\text{Ga}_{0.8}\text{As}/\text{GaAs}$  single QW, grown by molecular-beam epitaxy on (001) semi-insulating GaAs substrate, was studied by RDS. The structure of the sample is as follow: first a 2000-Å GaAs buffer layer, then ten periods of 50-Å GaAs/50-Å  $\text{Al}_{0.3}\text{Ga}_{0.7}\text{As}$  SL, then 5000-Å GaAs, then a 70-Å  $\text{In}_{0.2}\text{Ga}_{0.8}\text{As}$  QW, and finally an 1000-Å GaAs cap. All the epilayers were intentionally undoped, but residual doping gives rise to a small field in the surface depletion region. The sample was placed in a variable-temperature cryostat for RDS measurements from 300 to 80 K. The reflectance difference between the  $[110]$  and the  $[1\bar{1}0]$  directions was measured by the Fourier-transform RDS setup.<sup>3</sup> Fourier-transform photoreflectance (PR), where the probe beam was from the Fourier-transform spectrometer and the excitation was from an Ar-ion laser chopped at 16 KHz, was also carried out at room temperature to identify the allowed transitions.

Given the width of this  $\text{In}_{0.2}\text{Ga}_{0.8}\text{As}$  QW, there are three allowed transitions and three forbidden transitions from the five subbands: one LH subband (1L), two HH subbands (1H,2H), and two electron subbands (1E,2E). The three allowed transitions are easily observed by PR at room temperature [the bottom curve in Fig. (1)]. Three peaks (peak A at 1.260 eV, B at 1.334 eV, and C at 1.386 eV) below the sharp structure at 1.421 eV of the GaAs band edge are clearly seen. The three peaks are assigned to the 1H1E (the transition from 1H to 1E), the 1L1E, and the 2H2E transitions, respectively. Our calculations of the subband energies confirm this assignment. In addition, we note that there are a few Franz-Keldysh oscillation (FKO) peaks above the GaAs band edge, indicating that there is a residual electric field in the sample. From the FKO the residual electric field is found to be 4.6 kV/cm. In such a small field, the parities of the

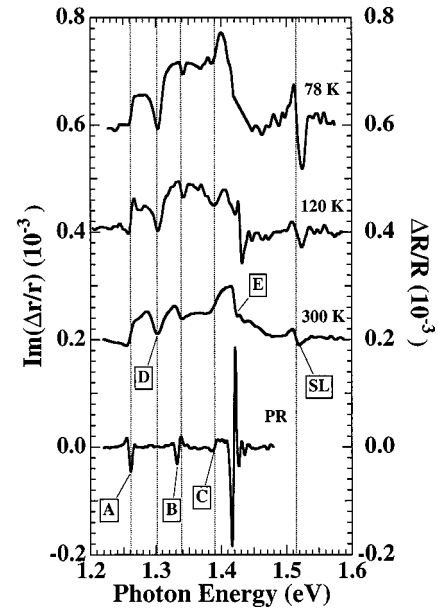


FIG. 1. The photoreflectance spectrum (bottom curve, right axis) and the reflectance-difference (RD) spectra (top three curves, left axis) of an  $\text{In}_{0.2}\text{Ga}_{0.8}\text{As}$  quantum well. The RD spectrum at 120 K has been shifted horizontally by  $-62$  meV, and that at 80 K has been shifted by  $-76.5$  meV. The RD spectra at 300, 120, and 78 K have also been vertically shifted by 0.0002, 0.0004, and 0.0006, respectively.

subband wave functions are well maintained and the forbidden transitions are very weak. That is why no forbidden transition was observed by PR.

The three top curves in Fig. 1 show the imaginary RD spectra measured at room temperature, 120 and 78 K, respectively. The imaginary RD spectra,  $\text{Im}(\Delta r/r)$ , is proportional to the anisotropy of the transition probability,  $\Delta M$  [ $\sim \text{Im}(\Delta \epsilon)$ ], because the cap layer introduces a phase factor<sup>3</sup> very close to  $-i$ . Besides the three structures corresponding to the three allowed transitions (A,B,C) in PR, two new structures, D and E, appear, together with the structure “SL” at 1.515 eV. The latter is related to the 1H1E and the 1L1E transitions of the GaAs/ $\text{Al}_x\text{Ga}_{1-x}\text{As}$  SL, and we will not discuss it in detail here. The structure D, which is absent in the PR spectrum, is believed to arise from the 2H1E transition according to its energy position confirmed by calculations. The structure E located near 1.421 eV is due to the 1L2E transition. There are two reasons: (1) the energy difference between E and C (about 35 meV) is nearly the same as that between D and B (37 meV); (2) its anisotropy amplitude is approximately equal to that of C (2H2E) except with a negative sign. This feature is verified by calculations shown later. The five resonances have distinct signs, i.e., structures A and C are of the same sign, and that of B, D, and E are all opposite of that of A and C.

The observed RDS structures cannot be due to the normal Pockels effect of the residual field.<sup>8</sup> As has been discussed above, this is because the electric field only couples the HH and the LH subbands with the same parity, i.e., 1H to 1L in the QW. This can only explain the anisotropy of the 1H1E and the 1L1E transitions. The strong anisotropy of the 2H1E transition implies that there is strong coupling between the 2H and the 1L subbands, which is made possible by the IP.

TABLE I. Optical transition anisotropy of the  $\text{In}_{0.2}\text{Ga}_{0.8}\text{As}$  quantum well observed by reflectance-difference spectroscopy and calculated by  $\mathbf{K}^*\mathbf{P}$  theory with and without the interface potential. The data in the last two rows are for the  $\text{GaAs}/\text{Al}_{0.3}\text{Ga}_{0.7}\text{As}$  superlattice. The  $\Delta r/r$  of the superlattice has been corrected for the absorption of the top GaAs and  $\text{In}_x\text{Ga}_{1-x}\text{As}$  layers.

Transitions	Experiments		Theory			
	Energy (eV)	$\Delta r/r(10^{-5})$	Energy (eV)	$\Delta r/r(10^{-5})$ (Pockels only)	$\Delta r/r(10^{-5})$ (Ivchenko's)	$\Delta r/r(10^{-5})$ (reduced IP)
1H1F (A)	1.260	5.4	1.263	0.88	12.3	4.75
1L1E (B)	1.334	-2.7	1.330	-0.83	-3.1	-2.37
2H2E (C)	1.386	5.0	1.383	0.01	23.9	9.96
2H1E (D)	1.297	-4.7	1.296	0.00	-8.8	-3.9
1L2E (E)	1.420	-5.9	1.417	0.02	-23.4	-9.43
1H2E		0	1.350	0.00	0.04	0.016
1H1E (SL)	1.510	3.4	1.509	2.35	16.4	
1L1E (SL)	1.520	-3.6	1.522	-2.33	-20.4	

The RDS amplitudes of all the transitions of this  $\text{In}_x\text{Ga}_{1-x}\text{As}$  QW are calculated in the framework of the  $\mathbf{K}^*\mathbf{P}$  theory, treating the IP given by Eq. (1) and the electric field as a perturbation. Table I shows the RDS strength measured at room temperature and the calculated results. The absorption due to the cap layer has been corrected. For Krebs model  $\text{VBO}=58\text{ meV}$  was taken for the  $\text{In}_{0.2}\text{Ga}_{0.8}\text{As}/\text{GaAs}$  interface. The value of  $P_0$  for Ivchenko's model for  $\text{InAs}/\text{GaAs}$  is about the same as Krebs based on a simple tight-binding estimation. The results are for zero in-plane wave vector. From the table, we see that the RDS signs of all the observed transitions (including 1L2E) are reproduced exactly if the IP is taken into account. The anisotropy intensity of the 2H1E and the 1L2E forbidden transitions are comparable to that of the 1H1E and the 1L1E allowed transitions. The 2H2E transition anisotropy is about the same as that of the 1L2E transition except with an opposite sign, while that of the 1H2E transition is very small. The reason for the latter to be small is because there is no 2LH subband in the QW to couple with the 1HH through the interface anisotropy potential. If we change the sign of the IP strength, the signs of all the transitions will be reversed. The amplitudes of the forbidden transitions will remain the same while that of the allowed transitions, due to the Pockels effect, will be changed. The amplitudes and the signs of the anisotropy of all the allowed and forbidden transitions predicted by theory are qualitatively consistent with the experimental results, if the IP is included. If the IP is ignored, then only two anisotropic structures associated with the 1H1E and the 1L1E transitions should be present. This is clearly in contradiction with the experimental results.

We now discuss briefly the line shape of the RDS structures. It is noted that only the 1H1E transition shows a clear step-function line shape, which reflects the two-dimensional nature of the joint density of states of the transition. The line shapes of other transitions are more peaklike (positive or negative). This is very clear for the 2H1E (structure *D*) transition. To consider the lineshape involves nonzero in-plane wave vector ( $q \neq 0$ ), which couples the  $|\frac{3}{2}, +\frac{3}{2}\rangle$  and the  $|\frac{3}{2}, +\frac{1}{2}\rangle$  states (or  $|\frac{3}{2}, +\frac{3}{2}\rangle$  and  $|\frac{3}{2}, -\frac{1}{2}\rangle$ ) through  $\partial/\partial z$ . Its average value can be of the order of  $1/a$  ( $a$  is the width of QW) when the envelope functions of the coupled HH and LH subbands

have different parities, and is close to zero for subbands with the same parity. This coupling does not contribute to the transition anisotropy because the  $|\frac{3}{2}, +\frac{3}{2}\rangle$  and the  $|\frac{3}{2}, +\frac{1}{2}\rangle$  states have different spins. Instead, it reduces the existing coupling between the  $|\frac{3}{2}, +\frac{3}{2}\rangle$  and the  $|\frac{3}{2}, -\frac{1}{2}\rangle$  states by transferring oscillation strength from it, therefore reducing the transition anisotropy. The coupling between the  $|\frac{3}{2}, +\frac{3}{2}\rangle$  state of the 2H subband and the  $|\frac{3}{2}, -\frac{1}{2}\rangle$  state of the 1L subband caused by the IP, which produces the transition anisotropy, is decreased by the coupling between the  $|\frac{3}{2}, +\frac{3}{2}\rangle$  state of the 2H subband and the  $|\frac{3}{2}, +\frac{1}{2}\rangle$  state of the 1L subband due to  $q \neq 0$ . As a result, the RDS amplitudes decrease according to  $[1 - (E - E_0)/\Delta E]$  for the transitions that involve the coupling caused by  $q \neq 0$ . Here  $E_0$  is the transition energy at  $q=0$ ,  $E$  is the photon energy,  $\Delta E$  is proportional to the square of the QW width and the square of the energy difference between the coupled hole subbands. For the 2H1E transition  $\Delta E = 30\text{ meV}$ , which is comparable to the actual line width of  $D$ . The line shape confirms again that the anisotropy of the 2H1E transition indeed comes from the coupling between the 2H and the 1L subbands caused by the IP.

The two IP models can explain qualitatively the experimental results. To quantitatively compare the models with the RD structures, we first need to address the issue of joint density of states of the electronic transitions between the QW subbands used in the calculations.

First, we adopt the experimental values of the in-plane effective mass of the first 1E and the 1H subbands,<sup>10,11</sup>  $m_{1H}(=0.14)$  and  $m_{1E}(=0.071)$ , in the unit of free-electron mass. Next, we take the estimated value of 0.065 (=bulk value for GaAs) for the 2E subband mass, because the value of  $m_{1E}$  is already quite close to the bulk value. In the absorption spectra<sup>12</sup> of  $\text{In}_x\text{Ga}_{1-x}\text{As}$  QW's, the absorption strength of the 1H1E transition is twice of the 1L1E one. Since the theoretical transition probability ratio of the two is 3 to 1, the joint density of 1L1E is then 1.5 times the 1H1E transition, or 0.07. In other words, the 1L mass is much larger than the 1E one, which is expected. Furthermore, the experimental absorption strength<sup>12</sup> of 2H2E is comparable to that of the 1H1E, and the theoretical transition probability of 2H2E is 0.67 times that of the 1H1E. This leads to the joint density of 0.07 for the 2H2E transition. Since this value is close to that

of the 2E mass, the mass of the 2H subband is also quite high, which is again expected from theoretical calculations. With the masses of all the subbands known, the joint density of the 1L2E and the 2H1E can be easily calculated.

We now compare the intensity ratio of the observed transitions with the calculated values using the IP models. Note that the intensity ratio is no longer dependent on the electric field, as long as it is small. This eliminates the uncertainty due to possible nonuniformity of the field. The calculated ratio of the 1H1E transition over the 1L1E one,  $R(1H1E/1L1E)$ , is about twice of the experimental one. This can be improved if we reduce the IP strength, since both transitions include the Pockels and the IP effects. The last column of Table I shows the calculated results using an IP strength 0.4 times of the original models. These results are much closer to the experimental ones than the ones using the full strength of IP.

Another quantitative discrepancy between theory and experiment is the relative strength of the two forbidden transitions. It is seen from Table I that the experimental value of the strength ratio  $R(1L2E/2H1E)$  is 1.26, while that of the theory is 2.66. Large discrepancy also exists for  $R(2H1E/2H2E)$ . Note that the ratio is independent of the electric field strength and the IP strength, if the potential takes the form given by Eq. (1). This suggests that the existing models, which describe the IP only in terms of the heavy-light-hole coupling, cannot fully explain the observed optical anisotropy. Coupling involving other bands, which have not been addressed by these models, may also play an important role. By taking into account the coupling involving these bands, one may be able to change the relative strength of these transitions, because the contributions of the new coupling are different for different transitions.

One immediate candidate of additional coupling is the one involving the nearby  $\Gamma_7$  band. There are two aspects of the  $\Gamma_7$ -band coupling. First, each  $\Gamma_8$  subband contains a small component of the  $\Gamma_7$  band wave function. However, since this component is much smaller than that of the  $\Gamma_8$  band, the anisotropy it induces, if there is any, will also be much smaller than that of the  $\Gamma_8$  band, and change little the final results. The second is the  $\Gamma_7$ - $\Gamma_8$ -band coupling in the IP. By the symmetry argument, the coupling strength of heavy-light hole of the  $\Gamma_8$  band is of the same order of magnitude as the  $\Gamma_7$ - $\Gamma_8$  one, but the energy separation of the  $\Gamma_8$  subbands ( $\sim 10$  meV) is much smaller than the ones between  $\Gamma_7$ - $\Gamma_8$  one ( $\sim 300$  meV). The contribution of the  $\Gamma_7$  band to the anisotropy through IP will again be much smaller than the heavy-light-hole coupling. Therefore, coupling involving the  $\Gamma_7$  will change little the calculated relative strength. Similar argument can be applied to the coupling involving the  $\Gamma_6$  conduction band. Only the coupling involving other bands such as the  $L$  and/or  $X$  bands with considerable strength could change the relative strength of the transitions, but the exact formula is still not available at present.

In conclusion, clear experimental evidences for the existence of the IP at common-atom semiconductor interfaces are presented. The observed RDS transitions in an  $\text{In}_{0.2}\text{Ga}_{0.8}\text{As}/\text{GaAs}$  QW can be qualitatively explained when the IP is included in the  $\mathbf{K}^*\mathbf{P}$  model. The theoretical value of the anisotropy strength ratio involving the two forbidden transitions is two times larger than the observed one. This suggests that the existing IP models are not sufficient to fully explain the observed optical anisotropy. Effects due to coupling involving the  $X$  and/or  $L$  bands may also play an important part. The observed strength of the IP is about 0.4 times the theoretical one. More studies are underway to further explore the properties of the interfaces.

<sup>1</sup>E. L. Ivchenko and A. Yu. Kaminski, Phys. Rev. B **54**, 5852 (1996).

<sup>2</sup>O. Krebs and P. Voisin, Phys. Rev. Lett. **77**, 1829 (1996).

<sup>3</sup>Z. Yang, I. K. Sou, Y. H. Yeung, G. K. L. Wong, J. Wang, C. X. Jin, and X. Y. Hou, J. Vac. Sci. Technol. B **14**, 2973 (1996).

<sup>4</sup>W. Seidal, P. Voisin, J. P. Andre, and F. Bogani, Solid-State Electron. **40**, 729 (1996).

<sup>5</sup>O. Krebs, W. Seidel, J. P. Andre, D. Bertho, C. Jouanin, and P. Voisin, Semicond. Sci. Technol. **12**, 938 (1997).

<sup>6</sup>L. Vervoort, R. Ferreira, and P. Voisin, Phys. Rev. B **56**, R12 744 (1997).

<sup>7</sup>S. H. Kwok, H. T. Grahn, K. Ploog, and R. Merlin, Phys. Rev.

Lett. **69**, 973 (1992).

<sup>8</sup>O. Krebs, D. Rondi, J. L. Gentner, L. Goldstein, and P. Voisin, Phys. Rev. Lett. **80**, 5770 (1998).

<sup>9</sup>Y. H. Chen, Z. Yang, Z. G. Wang, B. Xu, J. B. Liang, and J. J. Qian, Phys. Rev. B **56**, 6770 (1997).

<sup>10</sup>E. D. Jones, S. K. Lyo, I. J. Fritz, J. F. Klem, J. E. Schirber, C. P. Tigges, and T. J. Drummond, Appl. Phys. Lett. **54**, 2227 (1989).

<sup>11</sup>Yu-Lin Shawn, H. P. Wei, D. C. Tsui, and J. F. Klem, Appl. Phys. Lett. **67**, 2170 (1995).

<sup>12</sup>W. Z. Shen, W. G. Tang, S. C. Shen, S. M. Wang, and T. Andersson, Appl. Phys. Lett. **65**, 2728 (1994).